

## New Phytologist Supporting Information

Article title: Genomic imprints of unparalleled growth

Authors: Omer Murik, Or Geffen, Yoram Shotland, Noe Fernandez-Pozo, Kristian Karsten Ullrich, Dirk Walther, Stefan Andreas Rensing and Haim Treves

Article acceptance date: 31 October 2023

The following Supporting Information is available for this article:

**Fig. S1** *Ohadii* genome phylogenetic analysis A. Bayesian inference phylogenetic tree generated by MrBayes with preset mixed amino acid rate matrices, based on the amino acids sequences of 495 single copy BUSCO genes present in all species, concatenated and aligned with MAFFT. Highest Posterior Density values, resulting from 500,000 generations, are shown at the nodes. The tree is rooted using *C. reinhardtii* as outgroup. B. Venn diagram of *Ohadii* genes with homologues in other *Chlorella* spp.

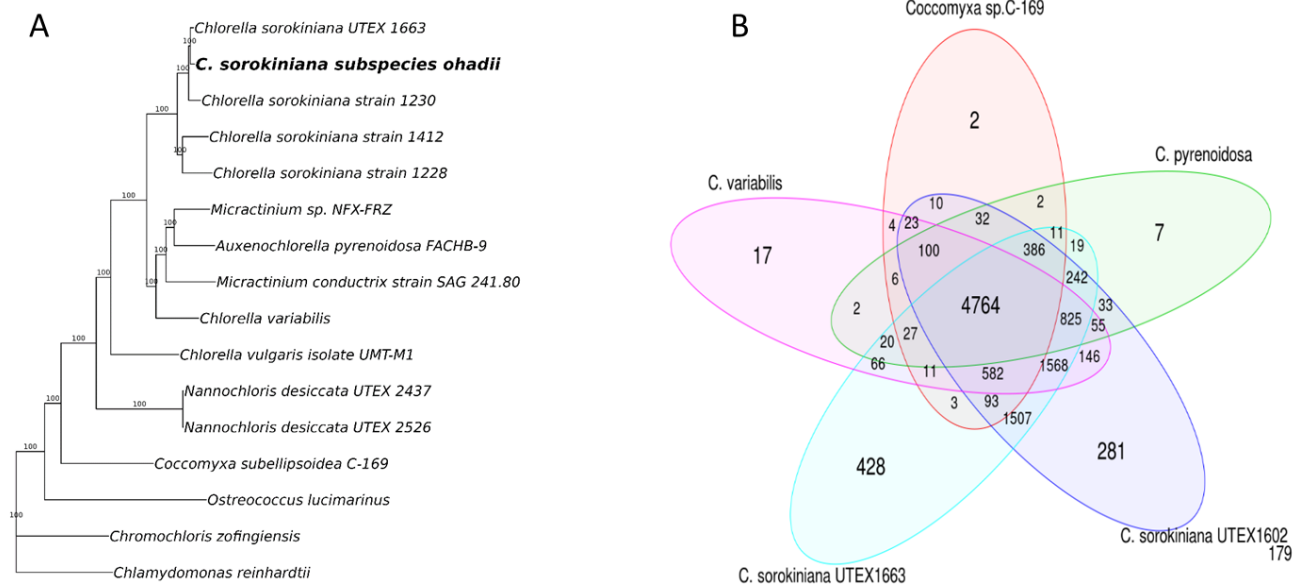


**Fig. S2** Calculated Ka/Ks values for different GO biological process terms in several *Chlorella* spp. (A. *pyrenoidosa*, *C. variabilis*, *C. sorokiniana* and *C. subellipsoidea*).

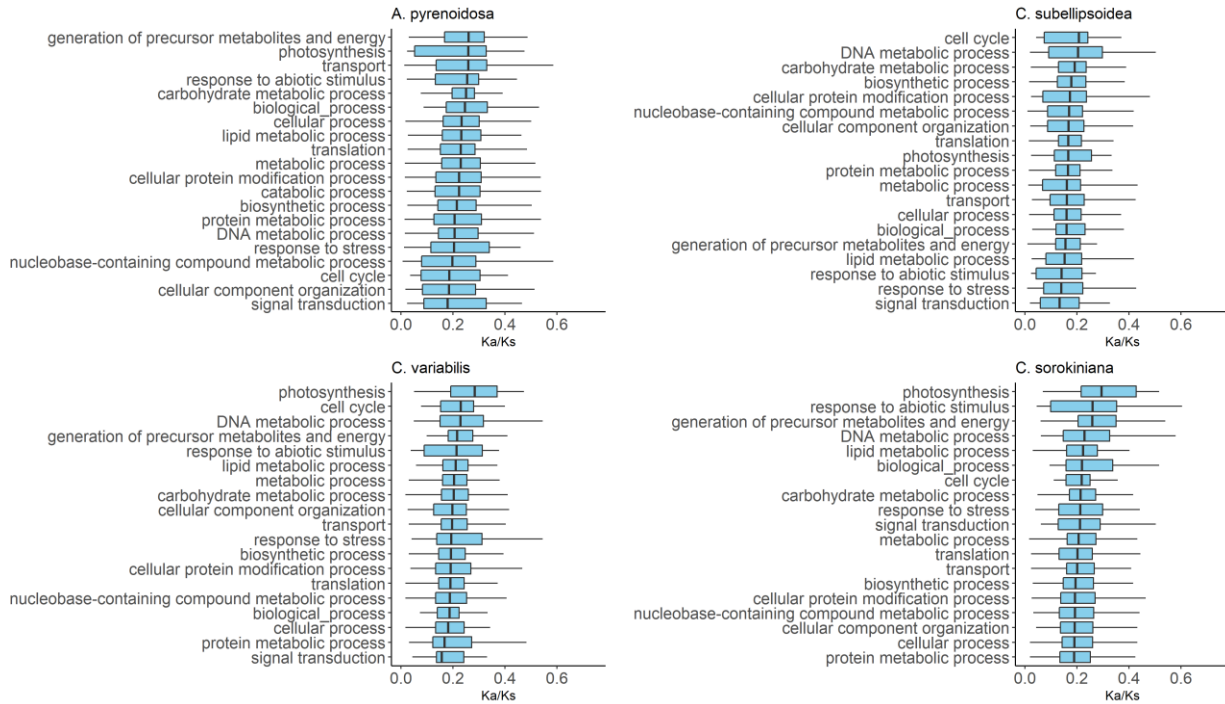


**Fig. S3** Provided as a separate SI file due to size.

**Fig. S4** In silico estimation of rDNA copy number in the genomes of several algal species. Copy number was estimated by dividing the average coverage of raw genomic DNA sequencing reads within the ribosomal genes region by the overall average coverage. For *Ohadii*, the copy number was also validated by qPCR (see methods). To normalize estimated copy numbers on cell volume we used published data (see SI text) on cell diameters of presented species for cell volume estimation, assuming spherical shape for simplicity. Normalized values represent estimated rDNA copy per cell volume ( $\mu\text{m}^3$ ).

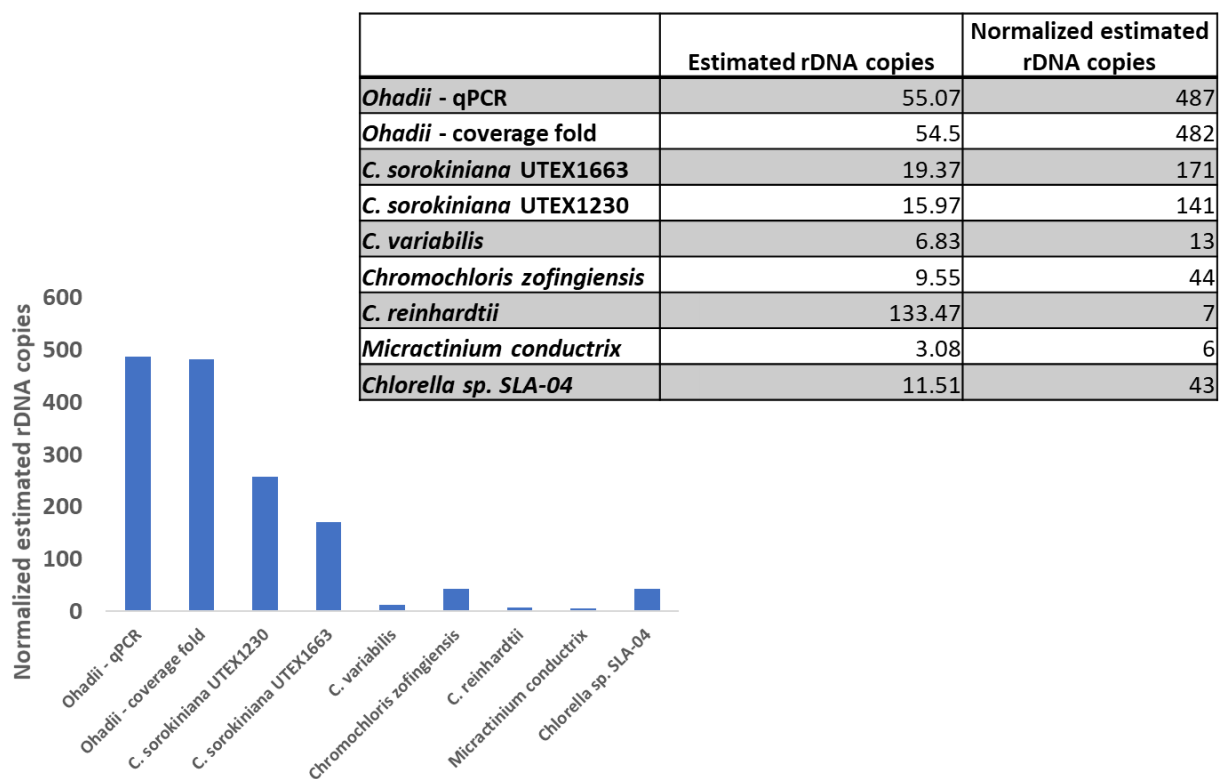


**Fig. S5** Transcript abundance, expressed as FPKM values of mixotrophically grown *Ohad* cells, as a function of intron density (number per kb transcript). Each dot represents a single gene. Benjamini-Hochberg adjusted p-value= $2.5 \times 10^{-168}$ , Pearson correlation.

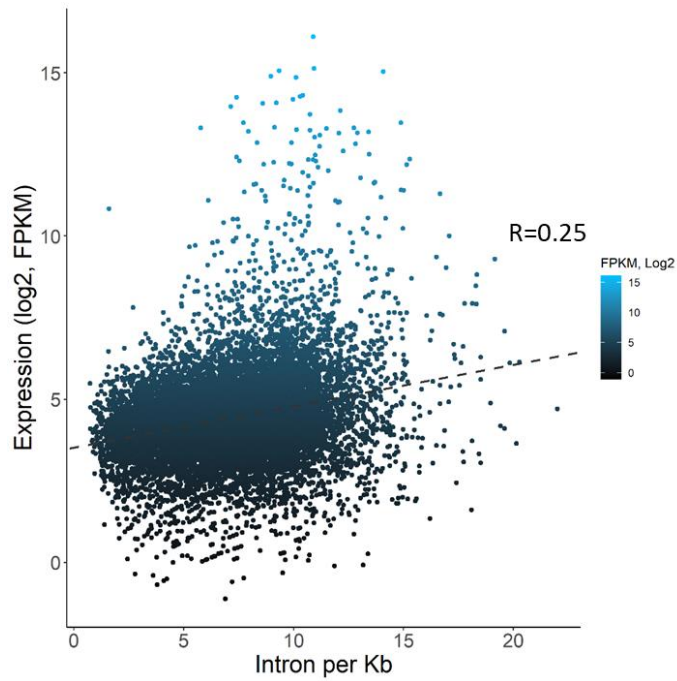


**Fig. S6** Boxplot of gene expression values ( $\log(\text{FPKM}+0.1)$ ) vs. all parameter combinations: medium (mixo-/autotroph), light (high/ low, HL/LL), and intron density (high/medium/low, HD/MD/LD). Intron density was binned into low/medium/high based on the 1/3 and 2/3 quantiles of the respective intron densities (number of introns per kb mRNA).

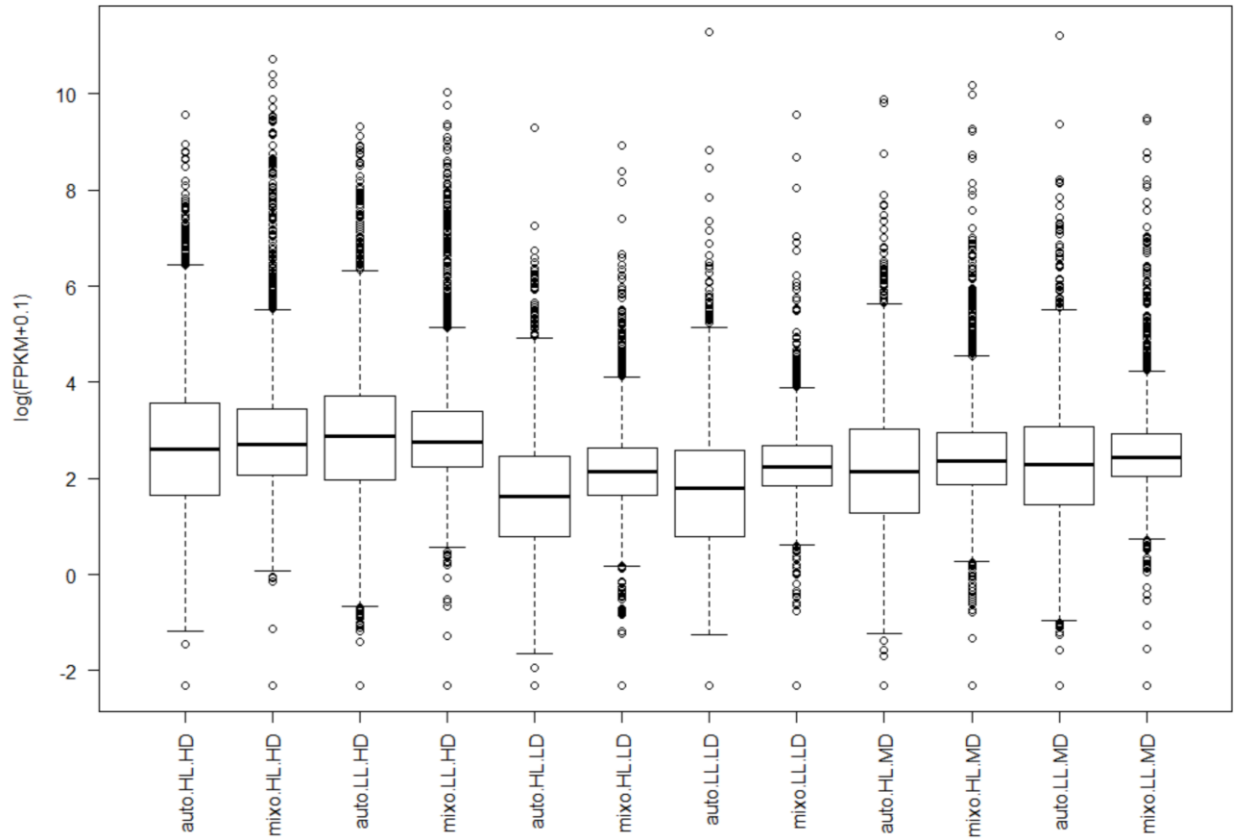


**Fig. S7** Comparative intron abundance analysis of *Chlorella* spp. A-B. Boxplots representing the difference in the number of introns per gene between *Ohadii* genes and their orthologue in *C. subellipsoidosa* and *C. sorokiniana* 1663, respectively, based on different GO terms. C. IPG distribution across *Ohadii*, *C. sorokiniana* 1663 and *C. subellipsoidosa* genomes. Dashed lines denote per-species median values.

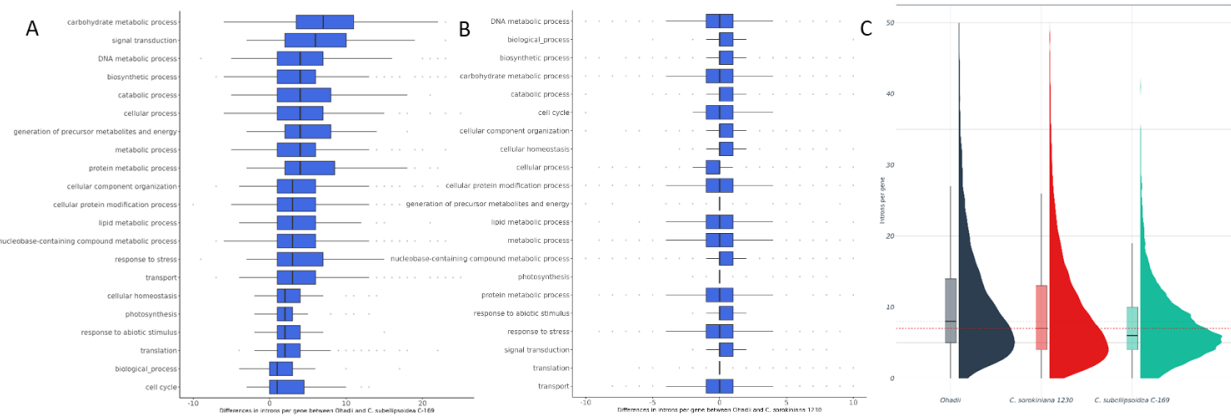
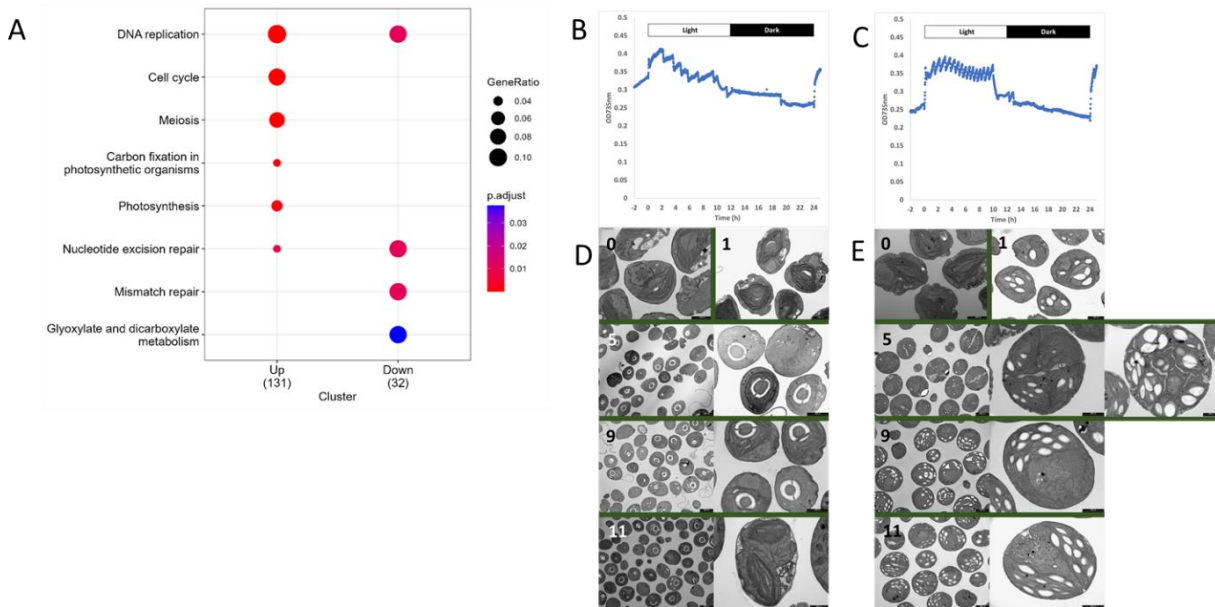


**Fig. S8** Effect of C level on *Ohad* vegetative cell cycle. (A) Enriched GO terms among up- or downregulated genes in autotrophically (TP) compared with mixotrophic (TAP) *Ohad* cultures. (B-E) *Ohad* continuous (turbidostat) cultures were grown autotrophically under diurnal cycles (12/12) of saturating light, either with ambient (B) or 5% CO<sub>2</sub> (C). Note the higher frequency of dilution events on High-CO<sub>2</sub> cultures caused by the faster growth rate. (D and E) TEM images of cell cultures corresponding to A and B, respectively along time points (in hours) starting from transition from dark to light. Note the well-developed pyrenoids in Low-CO<sub>2</sub> cells (D) and the larger diameter and starch content in High-CO<sub>2</sub> (E). Bars indicate 2000 and 1000 nm in the left and right images in each panel, respectively.





**Tables S1, S3, S4, S6, S7 and S9-S14** are provided in a separate excel file due to size, with their legends detailed below.

**Table S1** Expression profiles of all 11,407 *Ohad* genes under various conditions. Note that this table was presented and discussed in an earlier study (Treves et al., 2020). It is provided here again for the comprehensiveness of the data set and the convenience of the reader while analysing the data.

**Table S3** BLAST, eggNOG, GO, KEGG and KOG annotations for all 11,407 *Ohad* genes.

**Table S6** Ribosomal proteins associated gene expression under EIL

**Table S7** Introns per gene in *Ohad* and *C. variabilis* genomes.

**Table S9A** orthologues groups and the number of genes belonging to each group in several algal genomes.

**Table S9B** Prohibitin genes and EIL expression. Asterisks denote mitochondrial localization prediction.

**Table S10** List of orphan genes found in *Ohad* genome with no detectable orthologue in all publicly available genomes, including or excluding the *C. sorokiniana* UTEX1663 genome published here.

**Table S11** Transcription associated proteins in *Ohad* genome.

**Table S12** Genome accessions used for phylogenetic analysis and comparative genomics in this study.

**Table S13** Cell cycle associated gene expression.

**Table S14** Glutamine content per protein in *Ohad* and in orthologous proteins in other algae.

**Table S2** *Ohad* gene annotation statistics and QC parameters.

<b>Transcripts with start / stop codons</b>	11296 (98.6%) / 11326 (98.8%)
<b>Genes with RNAseq evidence (FPKM&gt;3)</b>	10685 (96.7%)
<b>Genes with BLAST hit</b>	9640 (87.2%)
<b>Genes with GO annotation</b>	8514 (77.1%)
<b>Genes with InterProScan hit</b>	8086 (73.2%)
<b>Genes with KEGG annotation</b>	4460 (40.3%)
<b>Genes with eggNOG hit</b>	8384 (76%)

**Table S5** Output of the RepeatMasker tool for the assembly of the *Ohadii* genome.

	NUMBER OF ELEMENTS	LENGTH OCCUPIED (BP)	PERCENTAGE OF SEQUENCES OF GENOME	PERCENTAGE OF SEQUENCES OF TOTAL REPEATS
<b>RETROELEMENTS</b>	<b>330</b>	<b>39246</b>	<b>0.07</b>	<b>1.38</b>
<b>LINES:</b>	89	11588	0.02	0.41
R2/R4/NESL	11	1737	0.00	0.06
RTE/BOV-B	15	1354	0.00	0.05
L1/CIN4	62	8440	0.01	0.30
<b>LTR ELEMENTS:</b>	241	27658	0.05	0.97
TY1/COPIA	78	10620	0.02	0.37
GYPSY/DIRS1	163	17038	0.03	0.60
<b>DNA TRANSPOSONS</b>	<b>47</b>	<b>4659</b>	<b>0.01</b>	<b>0.16</b>
TC1-IS630-POGO	30	3026	0.01	0.11
OTHER(MIRAGE, P-ELEMENT, TRANSIB)	2	211	0.00	0.01
<b>UNCLASSIFIED:</b>	<b>1</b>	<b>116</b>	<b>0.00</b>	<b>0.00</b>
<b>TOTAL INTERSPERSED</b>		<b>44021</b>	<b>0.08</b>	<b>1.55</b>
<b>SMALL RNA:</b>	<b>14</b>	<b>8662</b>	<b>0.02</b>	<b>0.30</b>
<b>SATELLITES:</b>	<b>0</b>	<b>0</b>	<b>0.00</b>	<b>0.00</b>
<b>SIMPLE REPEATS:</b>	<b>49408</b>	<b>2642039</b>	<b>4.61</b>	<b>92.90</b>
<b>LOW COMPLEXITY:</b>	<b>2114</b>	<b>105351</b>	<b>0.18</b>	<b>3.70</b>
<b>TOTAL</b>		<b>2844094</b>	<b>4.97</b>	<b>100.00</b>
<b>TOTAL GENOME</b>		<b>57253654</b>		

**Table S8** Three-way ANOVA analysis with interaction effects of gene expression levels ( $\log(\text{FPKM}+0.1)$ ). Tested parameters: parameter combinations: medium (mixo/autotroph), light (high/ low, H/LL), and intron density (high/medium/low, H/M/LD). Intron density was binned (“IntronDensBinned”) based on the 1/3 and 2/3 quantiles of the respective intron densities (number of introns per kb mRNA). When using continuous intron-densities, qualitatively similar results were obtained (not shown).

	<b>Df</b>	<b>Sum Sq</b>	<b>Mean Sq</b>	<b>F value</b>	<b>Pr (&gt;F)</b>
<b>IntronDensBinned</b>	2	5832	2915.9	1607.681	$< 2e^{-16}$
<b>Medium</b>	1	1925	1925.2	1061.473	$< 2e^{-16}$
<b>Light</b>	1	5	4.6	2.563	0.109366
<b>IntronDensBinned:Medium</b>	2	341	170.4	93.968	$< 2e^{-16}$
<b>IntronDensBinned:Light</b>	2	8	3.8	2.090	0.123675
<b>Medium:Light</b>	1	24	23.9	13.151	0.000288
<b>IntronDensBinned:Medium:Light</b>	2	25	12.4	6.864	0.001046

**Table S12** Genome accessions used for phylogenetic analysis and comparative genomics in this study.

<b>Organism</b>	<b>Accession</b>	<b>Version</b>
<b>Arabidopsis thaliana</b>	GCF_000001735.4	TAIR10
<b>Auxenochlorella pyrenoidosa</b>	GCA_001430745.1	Strain FACHB-9, v1.0
<b>Botryococcus braunii</b>	GCA_002005505.1	Strain Showa, v1.0
<b>Chlamydomonas reinhardtii</b>	GCA_000002595.3	v5.5
<b>Ohadii</b>	This study	
<b>Chlorella sorokiniana UTEX1602</b>	GCA_002245835.2	v2.0
<b>Chlorella sorokiniana UTEX1663</b>	This study	
<b>Chlorella variabilis</b>	GCF_000147415.1	Strain NC64A, v1.0
<b>Chromochloris zofingiensis</b>	Phytozome ID 461	v.5.2.3.2
<b>Coccomyxa subellipsoidea C-169</b>	GCF_000258705.1	v2.0
<b>Micromonas pusilla CCMP1545</b>	GCF_000151265.2	v2.0
<b>Ostreococcus lucimarinus</b>	GCF_000092065.1	Strain CCE9901, v1.0
<b>Volvox carteri</b>	GCF_000143455.1	Strain Eve, v1.0

### Notes S1 Orphan Genes

An additional interesting example for an orphan gene can be found in the case of DNA polymerase zeta (Pol  $\zeta$ ), which is involved in translesion DNA synthesis and thus considered a driving force of evolution (Tamuli and Kasbekar, 2008). Both N- and C-termini of Pol  $\zeta$  (encoded by g8142) are similar to those present in other organisms, but the closest ortholog (*C. sorokiniana*) is 1,981 AA long, compared with 2,825 AA in *Ohadii*. The central part in *Ohadii*'s Pol  $\zeta$  shows no similarity to a known gene, but is characterized by intrinsically disordered regions and stretches of glutamine residues (see below). Incidentally, the 2,815 AA in Pol  $\zeta$  from *Physcomitrella patens* also harbour a large unrecognized central part, not homologous to that found in *Ohadii*. While we cannot predict *Ohadii*'s Pol  $\zeta$  intrinsically disordered regions function and origin, such proteins were implicated in the ability to withstand desiccation in both eukaryotic (Boothby et al., 2017) and prokaryotic (Oren et al., 2019) organisms and may enable transcription under low water potential.

### Notes S2 Metabolic flexibility and polyamines

The unparalleled growth rate of *Ohadii* was, at least partly, attributed to its metabolic flexibility, i.e. its ability to shift between photoautotrophic (net O<sub>2</sub> evolution and CO<sub>2</sub> uptake) to photoheterotrophic (net O<sub>2</sub> uptake and CO<sub>2</sub> evolution) metabolism under otherwise constant conditions (Treves et al., 2017b, Treves et al., 2020). There are various aspects related to the metabolic shifts, here we focus on the involvement of polyamines and the sudden large enhancement of respiratory activity.

Our earlier studies implicated polyamines in the metabolic flexibility observed in *Ohadii* and its impact on the growth rate (Treves et al., 2017b, Treves et al., 2020). Thus, we searched for unique genes likely involved in polyamines metabolism in *Ohadii*. It is widely accepted that, like other eukaryotes, green algae depend on putrescine biosynthesis from ornithine since they have lost the arginine route towards polyamines (Fuell et al., 2010). To our surprise, bacterial originated genes, g4371 and g5694 (Table S4) encoding arginase and agmatinase are present and expressed (Table S1) in *Ohadii*. Agmatinase produces putrescine and urea from agmatine. Arginase cleaves arginine to form ornithine and urea. Its activity may enhance the supply of ornithine to the two ornithine decarboxylases (encoded by g6951 and g309) producing putrescine. Ubiquitin carboxyl-terminal hydrolases, encoded by g315 and g10824, respectively, may serve as an additional route to

polyamine biosynthesis in *Ohadii*. These are thiol enzymes that cleave conjugated ubiquitin thereby releasing ubiquitin and amide derivatives including spermidine (Pickart and Rose, 1985). Genes encoding ornithine decarboxylases, spermidine synthase and spermine oxidase are found in all *Chlorella* spp. examined here. On the other hand, the closest orthologues of g1053 encoding amine oxidase, potentially involved in polyamine degradation, are found in cyanobacteria but not in other green algae. Likely it was acquired by lateral gene transfer from a bacterial source. Noticeably, the transcript abundance of g75 encoding monoamine oxidase is among the highest in *Ohadii* (Table S1) but at this time it is unknown whether it is engaged in polyamine degradation. Altogether the unique genes identified here likely affect the rate of polyamine metabolism in *Ohadii* and thereby its metabolic flexibility and growth rate.

### **Notes S3** Light and C regulation of cell cycle in *Ohadii* cultures

Cell-cycle regulation represents an additional issue to consider regarding the growth of *Ohadii*, and especially under the unusual growth conditions in the BSC. We have previously referred to the unusual diurnal cycle in the crusts (Treves et al., 2020), and attributed *Ohadii*'s metabolic flexibility (Treves et al., 2017a), regulated by polyamines, to the need to operate within these temporal constraints (see Introduction and Results sections for several genomic aspects concerning polyamine metabolism). To explore the role played by cell-cycle regulators in controlling *Ohadii* growth under different abiotic conditions we examined their associated gene expression at several levels. At the functional level, we found no enrichment in GO terms associated with cell-cycle or cell-division in transcriptional response to different illumination levels, nor during a shift of *Ohadii* cultures from carbon-rich to low-carbon medium. On the other hand, differential gene-expression of cultures grown continuously on varying C regimes was over-represented with the GO terms 'Cell cycle' and 'DNA replication', exhibiting even more extensive response compared with genes associated with the GO terms 'Carbon fixation in photosynthetic organisms' and 'photosynthesis', directly related to the applied conditions (Figure S8A). Furthermore, manual examination of all genes associated with the GO groups of 'cell cycle' and 'cell division' in differential transcriptome analyses of *Ohadii* cultures under varying C levels, revealed up-regulation of cell-division inhibitors under low C regime, including the nuclear-encoded minE and FtsZ1, regulating chloroplast division (Miyagishima et al., 2012, Sumiya et al.,

2016), but not the plastid-encoded *minD* (Table S13). Chloroplast division, regulated by these genes, has been shown to be necessary for cellular division in algae. None of these genes exhibited transcriptional response to light, contrary to previous reports on the light response of *minD* in *C. vulgaris* (Miyagishima et al., 2012). This prompted us to examine the vegetative cell cycle of *Ohad战略ii* at different C levels (Figures S8B and S8C). We followed the morphology of *Ohad战略ii* continuous autotrophic cultures grown under 12/12-hour cycles of dark and saturating light ( $3000 \mu\text{mol photons m}^{-2} \text{s}^{-1}$ ) at low or high (5%)  $\text{CO}_2$  levels (Figures S8D and S8E, Respectively), isolating C level as a varying factor. In line with transcriptome data, whereas very few cells under low  $\text{CO}_2$  were captured under division, cells grown under high- $\text{CO}_2$  were larger, starch-rich and in many cases contained 2, 4 or even 16 daughter cells, especially at t5 and t11 hours (Figure S8E). This was also evident by the higher (~2-fold) number of dilution cycles in the latter (compare Figure S8C with S8B). As expected, most low- $\text{CO}_2$  grown cells exhibited a well-developed pyrenoid, a hallmark for the activation of algal CCM (Figure S8D). As both the availability of C for growth and the energetic costs of CCM operation (Burlacot et al., 2022, Burlacot and Peltier, 2023) likely underlie the difference in growth rate between the cultures, future work should implement a denser transcriptome time series under different C levels to reveal major regulators of *Ohad战略ii* vegetative growth.

#### **Notes S4** Comparative analysis of chloroplast- and mitochondrial-encoded genes

The *Ohad战略ii* chloroplast genome sequence assembles as a circular genome of 109,900 bp encoding a total of 111 genes, including 32 tRNA and one rRNA gene cluster consisting of 16S, 23S, and 5S rRNA genes (Figure S9A). The mitochondrial genome of *Ohad战略ii* is 52,560 in length, and consists of 60 genes, including 25 tRNA and the three rRNA genes (Figure S9B). With a G+C content of 34.01% and 29.14%, respectively, the chloroplast and mitochondrial genomes of *Ohad战略ii* are found within the range of other *Chlorella Spp* organellar genomes. Given the elevated growth and photosynthetic performance of *Ohad战略ii*, we sought to investigate changes in the sequence of plastid and mitochondrial encoded genes compared with other published algal genomes (Figure S9).

Most plastid genes encoding photosynthetic complexes subunits were highly conserved (>95% similarity) between *Ohad战略ii* variants and their homologues (Figure S9C). Exceptions were the PSI assembly factor encoding *ycf4* (Krech et al., 2012), the PSI antennae stabilizing unit encoding *psaJ*

(Schöttler et al., 2007), *psbJ*, encoding a PSII interacting unit regulating forward electrons flow downstream of  $Q_a^-$  (Ohad et al., 2004, Boussac et al., 2021), *petA*, encoding the *cytF* subunit of the *cytb6f* complex (Malone et al., 2021), and *psbT*, which has been shown to be required for PSII repair under EIL (Ohnishi et al., 2007, Fagerlund et al., 2020). Interestingly, the latter was among the few genes showing <99-100% similarity to its *C. sorokiniana* UTEX 1230 (Figure S9C).

Larger variance was demonstrated in plastid genes encoding RNA polymerase subunits, ribosomal proteins and genes encoding components of the sulfate/thiosulfate import system (Figure S9C). Most pronounced for the former was the *rpoC2* gene, encoding one of the core subunits of the plastid-encoded RNA polymerase (Börner et al., 2015). A similar trend could be observed for mitochondrial-encoded RNA polymerase subunits, ribosomal proteins genes (Figure S9D). However, contrary to photosynthetic complexes encoding genes, mitochondrial-encoded genes associated with the respiratory electron transport chain showed relatively large variation between *Ohadii* variants and their homologues.

#### **Notes S5** Mitochondrial Alternative Oxidase

Many of the genes involved in mitochondrial respiration such as malate dehydrogenase (g1256), NADH dehydrogenase (g4922), NADH:ubiquinone oxidoreductase (g626), NADH-cytochrome b5 reductase 1 (g8678) are strongly upregulated by EIL (Table S1). Of particular interest is the mitochondrial alternative oxidase (AOX) shown to dissipate excess redox and light energy in various photosynthetic organisms (Jiang et al., 2019, Kaye et al., 2019) and to affect the expression of chloroplast encoded genes in a diatom (Murik et al., 2019, Bailleul et al., 2015). In a recent study Grossman and colleagues showed an increased ROS accumulation and sensitivity to excess absorbed illumination in a *C. reinhardtii* mutant missing AOX. They suggested that coupling of chloroplast-mitochondria allows dissipation of photosynthetically derived electrons via AOX-dependent mitochondrial respiration (Kaye et al., 2019). *Ohadii* possesses two AOX encoding genes, g7312 and g8898. The latter was identified through homology with a recognized AOX in *C. reinhardtii* (Kaye et al., 2019). In addition, genes g5334, g8333, g8422, g8899 and g8900 showed high similarity to those annotated as AOX in *C. sorokiniana* UTEX1602 and *Micractinium conductrix* (sequence

IDs: PRW61073.1, PRW05807.1, [PSC70539.1](#) and [PSC73394.1](#)) but manual analyses could not confirm this annotation.

**Notes S6** Carbonic anhydrases and Bestrophin-like proteins involved in the CO<sub>2</sub> concentrating mechanism

The mechanisms whereby phytoplankton organisms raise the concentration of dissolved CO<sub>2</sub> in close proximity to Rubisco, and many of the genes involved, were largely recognized (Burnap et al., 2015, Brueggeman et al., 2012, Kaplan and Reinhold, 1999, Giordano et al., 2005, Mukherjee et al., 2019, Caspari et al., 2017, Mackinder et al., 2017, Beardall and Raven, 2020). Genes involved in inorganic carbon (Ci) uptake identified in *C. reinhardtii* are present in *Ohadii* where several other genes of unknown function are strongly upregulated under limiting carbon conditions (Table S1). Carbonic anhydrases (CA) perform essential parts in the operation of the CO<sub>2</sub> concentrating mechanism (CCM), stimulating the reversible interconversion between CO<sub>2</sub> and HCO<sub>3</sub><sup>-</sup> (Jensen et al., 2020). There are 12 genes encoding various CA types in *C. reinhardtii* (Jensen et al., 2020) compared with 17 genes in *Ohadii* (Table S3). Three of the five which belong to the Archaea  $\gamma$  type (Kupriyanova et al., 2017, DiMario et al., 2018, Moroney et al., 2011) (g3486, g7645, g7646, g9058 and g10488), are predicted to be mitochondria-located. At least six of the CA encoding genes are strongly upregulated under carbon limiting conditions, including two of the three predicted periplasmic-CAH1 encoded by g4440, g7577 and g9133.

In *Arabidopsis*, bestrophin-like proteins were implicated in voltage-dependent anion transport, including the chloroplast-located transporters (encoded by g870, g2082 and g3784 in *Ohadii*). They were also implicated in proton motive force and NPQ regulation upon transition of *Arabidopsis* from low light to EIL (Duan et al., 2016, Herdean et al., 2016). In *C. reinhardtii*, bestrophin-like proteins BST1-3 were recently shown to take part in HCO<sub>3</sub><sup>-</sup> transport into the thylakoid lumen as an essential part of the CCM (Mukherjee et al., 2019). Carbonic anhydrase accelerates the HCO<sub>3</sub><sup>-</sup> to CO<sub>2</sub> conversion in the pyrenoid confined thylakoid lumen raising its concentration in close proximity to Rubisco within these bodies (Kaplan and Reinhold, 1999, Giordano et al., 2005, Mukherjee et al., 2019, Caspari et al., 2017, Mackinder et al., 2017). There are 10 bestrophin-like proteins in *C. reinhardtii* (Mukherjee et al., 2019) compared with 20 in *Ohadii* (Table S3). Twelve

of them possess an UPF0187 motif suggesting chloroplast location. The transcript abundance of six of those - g2959, g6686, g7198, g7496, g8284 and g9777 is significantly upregulated under EIL and carbon limiting conditions (Table S1). Noticeably, the strongest upregulated gene among them, g7496, is located between two low CO<sub>2</sub> induced LCIB/C proposed to function as CO<sub>2</sub> to HCO<sub>3</sub><sup>-</sup> convertors thereby minimizing the loss of CO<sub>2</sub> (Mukherjee et al., 2019). LCIB/C were shown to interact with a bestrophin-like protein (Mackinder et al., 2017). The location and function of the other 8 bestrophin-like proteins in *Ohadii* is unknown. Interestingly, g9339 is among the fastest responding in redoxome experiments (Treves et al., 2020).

**Notes S7** The ascorbate glutathione cycle

Given the harsh conditions in its natural habitat, particularly EIL and desiccation, *Ohadii* must be able to cope with oxidative stress. Our earlier studies showed the involvement of the ascorbate/glutathione cycle in H<sub>2</sub>O<sub>2</sub> detoxification and in the induction of program cell death in *C. reinhardtii* with dehydroascorbate level acting as a surveillance mechanism for oxidative stress (Murik et al., 2014, Murik and Kaplan, 2009). There are eight genes encoding glutathione peroxidase in *Ohadii* (Table S3, g2924, g3526, g6722, g7601, g8725, g9383, g9401 and g10134), at least four of them are upregulated under EIL (Table S1). Five genes encode ascorbate peroxidase in *Ohadii* (g.27, g5287, g6985, g7865 and g10267). Among them g27 and g6985 were significantly upregulated under EIL and carbon limiting conditions. The annotation also recognized an ascorbate oxidase (g4623), dehydroascorbate reductase (g4290) and monodehydroascorbate reductase (g2209), the latter two are upregulated under EIL.

**Notes S8** Enrichment in glutamines and cysteines

Metabolic profiling revealed a large rise in glutamine (Q) level in *Ohadii* cells exposed to EIL (Treves et al., 2020). This prompted us to examine the abundance of Q residues in predicted protein sequences (Table S14). Long polyQ stretches were revealed in many predicted *Ohadii*'s proteins (such as Pol ζ mentioned above), particularly in orphan genes. To the best of our knowledge, little is known about the presence and role of polyQ in algae. They have been implicated in various diseases in primates, but their function is poorly understood (Mier and Andrade-Navarro, 2018). Generally, glutamine residues are more abundant in proteins of *Ohadii* and *C. sorokiniana* than in other

*Chlorella* spp., on average 30.3 residues per protein in *Ohadii*, but only 21.6 in *C. vulgaris*. In many cases, the orthologs of *Ohadii* genes bearing polyQ stretches show fewer Q residues or even none (Table S14). One example is g2082, encoding a component of chloroplast-located anion transporter, where long stretches of glutamine, the longest is 31 residues long close to the C-terminus, are clearly detected in *Ohadii*, but missing in an ortholog in *C. sorokiniana* UTEX 1602. Our analysis (TMHMM 2.0 (Krogh et al., 2001)) suggested seven transmembrane helices in g2082, and InterProScan also revealed a Zn-binding motif, suggesting involvement in gene regulation. Another example is the 23Q stretch in g6811, encoding a chloroplast-located ATP transporter in *Ohadii* but only 6Q in the *C. sorokiniana* UTEX1602 ortholog, and none in both *C. variabilis* and *C. reinhardtii*.

The *Ohadii* genome is also relatively rich in cysteine residues, 8-18% higher than in other algal species. This is observed in various ortholog groups, and in proteins that undergo redox regulation for instance in response to a shift in light intensity (Treves et al., 2020). A redoxome study, combined with a comparative genome analysis suggested the involvement of specific cysteines in the response of *Ohadii* to EIL (Treves et al., 2020). As an example, in *Ohadii*, the highly conserved C330 in the chloroplast-located NADP-malic dehydrogenase is substituted by isoleucine, likely resulting in a constitutive high activity of the enzyme (Treves et al., 2020). This is of particular importance for the export of redox from the chloroplast to the cytoplasm in EIL exposed cells.

## References

- BAILLEUL, B., BERNE, N., MURIK, O., PETROUTSOS, D., PRIHODA, J., TANAKA, A., VILLANOVA, V., BLIGNY, R., FLORI, S., FALCONET, D., KRIEGER-LISZKAY, A., SANTABARBARA, S., RAPPAPORT, F., JOLIOT, P., TIRICHINE, L., FALKOWSKI, P. G., CARDOL, P., BOWLER, C. & FINAZZI, G. 2015. Energetic coupling between plastids and mitochondria drives CO<sub>2</sub> assimilation in diatoms. *Nature*, 524, 366-369.
- BEARDALL, J. & RAVEN, J. A. 2020. *Acquisition of inorganic carbon by microalgae and cyanobacteria.*, Singapore, Springer.
- BOOTHBY, T. C., TAPIA, H., BROZENA, A. H., PISZKIEWICZ, S., SMITH, A. E., GIOVANNINI, I., REBECCHI, L., PIELAK, G. J., KOSHLAND, D. & GOLDSTEIN, B. 2017. Tardigrades Use Intrinsically Disordered Proteins to Survive Desiccation. *Molecular Cell*, 65, 975-984.e5.
- BÖRNER, T., ALEJNIKOVA, A. Y., ZUBO, Y. O. & KUSNETSOV, V. V. 2015. Chloroplast RNA polymerases: Role in chloroplast biogenesis. *Biochimica et Biophysica Acta (BBA) - Bioenergetics*, 1847, 761-769.
- BOUSSAC, A., SELLÉS, J., HAMON, M. & SUGIURA, M. 2021. Properties of Photosystem II lacking the PsbJ subunit. 2021.09.04.458961.

- BRUEGGEMAN, A. J., GANGADHARAI, D. S., CSERHATI, M. F., CASERO, D., WEEKS, D. P. & LADUNGA, I. 2012. Activation of the carbon concentrating mechanism by CO<sub>2</sub> deprivation coincides with massive transcriptional restructuring in *Chlamydomonas reinhardtii*. *The Plant Cell*, 24, 1860-1875.
- BURLACOT, A., DAO, O., AUROY, P., CUINÉ, S., LI-BEISSON, Y. & PELTIER, G. 2022. Alternative photosynthesis pathways drive the algal CO<sub>2</sub>-concentrating mechanism. *Nature*, 605, 366-371.
- BURLACOT, A. & PELTIER, G. 2023. Energy crosstalk between photosynthesis and the algal CO<sub>2</sub>-concentrating mechanisms. *Trends in Plant Science*.
- BURNAP, R. L., HAGEMANN, M. & KAPLAN, A. 2015. Regulation of the CO<sub>2</sub> concentrating mechanism in cyanobacteria. *Life*, (in press).
- CASPARI, O. D., MEYER, M. T., TOLLETER, D., WITTKOPP, T. M., CUNNIFFE, N. J., LAWSON, T., GROSSMAN, A. R. & GRIFFITHS, H. 2017. Pyrenoid loss in *Chlamydomonas reinhardtii* causes limitations in CO<sub>2</sub> supply, but not thylakoid operating efficiency. *J Exp Bot*, 68, 3903-3913.
- DIMARIO, R. J., MACHINGURA, M. C., WALDROP, G. L. & MORONEY, J. V. 2018. The many types of carbonic anhydrases in photosynthetic organisms. *Plant Sci*, 268, 11-17.
- DUAN, Z., KONG, F., ZHANG, L., LI, W., ZHANG, J. & PENG, L. 2016. A bestrophin-like protein modulates the proton motive force across the thylakoid membrane in *Arabidopsis*. *J Integr Plant Biol*, 58, 848-858
- ENGEL, B. D., SCHAFFER, M., KUHN CUELLAR, L., VILLA, E., PLITZKO, J. M. & BAUMEISTER, W. 2015. Native architecture of the *Chlamydomonas* chloroplast revealed by in situ cryo-electron tomography. *Elife*, 4.
- FAGERLUND, R. D., FORSMAN, J. A., BISWAS, S., VASS, I., DAVIES, F. K., SUMMERFIELD, T. C. & EATON-RYE, J. J. 2020. Stabilization of Photosystem II by the PsbT protein impacts photodamage, repair and biogenesis. *Biochimica et Biophysica Acta (BBA) - Bioenergetics*, 1861, 148234.
- FUELL, C., ELLIOTT, K. A., HANFREY, C. C., FRANCESCHETTI, M. & MICHAEL, A. J. 2010. Polyamine biosynthetic diversity in plants and algae. *Plant Physiology and Biochemistry*, 48, 513-520.
- GIORDANO, M., BEARDALL, J. & RAVEN, J. A. 2005. CO<sub>2</sub> concentrating mechanisms in algae: mechanisms, environmental modulation, and evolution. *Ann. Rev. Plant Biol.*, 56, 99-131.
- HERDEAN, A., TEARDO, E., NILSSON, A. K., PFEIL, B. E., JOHANSSON, O. N., ÜNNEP, R., NAGY, G., ZSIROS, O., DANA, S., SOLYMOSI, K., GARAB, G., SZABÓ, I., SPETEA, C. & LUNDIN, B. 2016. A voltage-dependent chloride channel fine-tunes photosynthesis in plants. *Nature Comm*, 7, 10.1038/ncomms11654.
- HIGUCHI, R., SONG, C., HOSHINA, R. & SUZAKI, T. 2018. Endosymbiosis-related changes in ultrastructure and chemical composition of *Chlorella variabilis* (Archaeplastida, Chlorophyta) cell wall in *Paramecium bursaria* (Ciliophora, Oligohymenophorea). *European Journal of Protistology*, 66, 149-155.
- JENSEN, E. L., MABERLY, S. C. & GONTERO, B., 21, 2922. 2020. Insights on the functions and ecophysiological relevance of the diverse carbonic anhydrases in microalgae. *Int. J. Mol. Sci*, 21, 2922.

- JIANG, Z. X., WATANABE, C. K. A., MIYAGI, A., KAWAI-YAMADA, M., TERASHIMA, I. & NOGUCHI, K. 2019. Mitochondrial AOX supports redox balance of photosynthetic electron transport, primary metabolite balance, and growth in *Arabidopsis thaliana* under high light. *Internl J Mol Sci*, 20.
- KAPLAN, A. & REINHOLD, L. 1999. The CO<sub>2</sub> concentrating mechanisms in photosynthetic microorganisms. *Annu. Rev. Plant Physiol. Plant Mol. Biol.*, 50, 539-570.
- KAYE, Y., HUANG, W. C., CLOWEZ, S., SAROUSSI, S., IDOINE, A., SANZ-LUQUE, E. & GROSSMAN, A. R. 2019. The mitochondrial alternative oxidase from *Chlamydomonas reinhardtii* enables survival in high light. *J Biol Chem*, 294, 1380-1395.
- KRECH, K., RUF, S., MASDUKI, F. F., THIELE, W., BEDNARCZYK, D., ALBUS, C. A., TILLER, N., HASSE, C., SCHÖTTLER, M. A. & BOCK, R. 2012. The plastid genome-encoded Ycf4 protein functions as a nonessential assembly factor for photosystem I in higher plants. *Plant Physiol*, 159, 579-91.
- KROGH, A., LARSSON, B., VON HEIJNE, G. & SONNHAMMER, E. L. 2001. Predicting transmembrane protein topology with a hidden Markov model: application to complete genomes. *J Mol Biol*, 305, 567-80.
- KUPRIYANOVA, E., PRONINA, N. & LOS, D. 2017. Carbonic anhydrase - a universal enzyme of the carbon-based life. *Photosynthetica*, 55, 3-19.
- LIZZUL, A. M., LEKUONA-AMUNDARAIN, A., PURTON, S. & CAMPOS, L. C. 2018. Characterization of *Chlorella sorokiniana*, UTEX 1230. *Biology (Basel)*, 7.
- MACKINDER, L. C. M., CHEN, C., LEIB, R. D., PATENA, W., BLUM, S. R., RODMAN, M., RAMUNDO, S., ADAMS, C. M. & JONIKAS, M. C. 2017. A spatial interactome reveals the protein organization of the algal CO<sub>2</sub>-concentrating mechanism. *Cell*, 171, 133-147.e14.
- MALONE, L. A., PROCTOR, M. S., HITCHCOCK, A., HUNTER, C. N. & JOHNSON, M. P. 2021. Cytochrome b6f – Orchestrator of photosynthetic electron transfer. *Biochimica et Biophysica Acta (BBA) - Bioenergetics*, 1862, 148380.
- MIER, P. & ANDRADE-NAVARRO, M. A. 2018. Glutamine Codon Usage and polyQ Evolution in Primates Depend on the Q Stretch Length. *Genome Biol Evol*, 10, 816-825.
- MIYAGISHIMA, S.-Y., SUZUKI, K., OKAZAKI, K. & KABEYA, Y. 2012. Expression of the Nucleus-Encoded Chloroplast Division Genes and Proteins Regulated by the Algal Cell Cycle. *Molecular Biology and Evolution*, 29, 2957-2970.
- MORONEY, J. V., MA, Y., FREY, W. D., FUSILIER, K. A., PHAM, T. T., SIMMS, T. A., DIMARIO, R. J., YANG, J. & MUKHERJEE, B. 2011. The carbonic anhydrase isoforms of *Chlamydomonas reinhardtii*: intracellular location, expression, and physiological roles. *Photosynth Res*, 109, 133-149.
- MUKHERJEE, A., LAU, C. S., WALKER, C. E., RAI, A. K., PREJEAN, C. I., YATES, G., EMRICH-MILLS, T., LEMOINE, S. G., VINYARD, D. J., MACKINDER, L. C. M. & MORONEY, J. V. 2019. Thylakoid localized bestrophin-like proteins are essential for the CO<sub>2</sub> concentrating mechanism of *Chlamydomonas reinhardtii*. *Proc Natl Acad Sci U S A*, doi: 10.1073/pnas.1909706116, 201909706.
- MURIK, O., ELBOHER, A. & KAPLAN, A. 2014. Dehydroascorbate: a possible surveillance molecule of oxidative stress and programmed cell death in the green alga *Chlamydomonas reinhardtii*. *New Phytol*, 202, 471-484.
- MURIK, O. & KAPLAN, A. 2009. Paradoxically, prior acquisition of antioxidant activity enhances oxidative stress-induced cell death. *Environ. Microbiol.*, 11, 2301-2309.

- MURIK, O., TIRICHINE, L., PRIHODA, J., THOMAS, Y., ARAUJO, W. L., ALLEN, A. E., FERNIE, A. R. & BOWLER, C. 2019. Downregulation of mitochondrial alternative oxidase affects chloroplast function, redox status and stress response in a marine diatom. *New Phytol*, 221, 1303-1316.
- OHAD, I., DAL BOSCO, C., HERRMANN, R. G. & MEURER, J. 2004. Photosystem II proteins PsbL and PsbJ regulate electron flow to the plastoquinone pool. *Biochemistry*, 43, 2297-308.
- OHNISHI, N., KASHINO, Y., SATOH, K., OZAWA, S.-I. & TAKAHASHI, Y. 2007. Chloroplast-encoded Polypeptide PsbT Is Involved in the Repair of Primary Electron Acceptor QA of Photosystem II during Photoinhibition in *Chlamydomonas reinhardtii*\*. *Journal of Biological Chemistry*, 282, 7107-7115.
- OREN, N., RAANAN, H., KEDEM, I., TURJEMAN, A., BRONSTEIN, M., KAPLAN, A. & MURIK, O. 2019. Desert cyanobacteria prepare in advance for dehydration and rewetting: The role of light and temperature sensing. *Molecular Ecology*, 28, 2305-2320.
- PICKART, C. M. & ROSE, I. A. 1985. Ubiquitin carboxyl-terminal hydrolase acts on ubiquitin carboxyl-terminal amides  
*J Biol Chem*, 260, 7903-7910.
- SALBITANI, G., BOLINESI, F., AFFUSO, M., CARRATURO, F., MANGONI, O. & CARFAGNA, S. 2020. Rapid and Positive Effect of Bicarbonate Addition on Growth and Photosynthetic Efficiency of the Green Microalgae *Chlorella Sorokiniana* (Chlorophyta, Trebouxiophyceae). *Applied Sciences* [Online], 10.
- SCHÖTTLER, M. A., FLÜGEL, C., THIELE, W., STEGEMANN, S. & BOCK, R. 2007. The plastome-encoded PsaJ subunit is required for efficient Photosystem I excitation, but not for plastocyanin oxidation in tobacco. *Biochem J*, 403, 251-60.
- SUMIYA, N., FUJIWARA, T., ERA, A. & MIYAGISHIMA, S.-Y. 2016. Chloroplast division checkpoint in eukaryotic algae. *Proceedings of the National Academy of Sciences*, 113, E7629-E7638.
- TAMULI, R. & KASBEKAR, D. P. 2008. Dominant Suppression of Repeat-Induced Point Mutation in *Neurospora crassa* by a Variant Catalytic Subunit of DNA Polymerase- $\zeta$ . *Genetics*, 178, 1169-1176.
- TREVES, H., MURIK, O., KEDEM, I., EISENSTADT, D., MEIR, S., ROGACHEV, I., SZYMANSKI, J., KEREN, N., ORF, I., TIBURCIO, A. F., ALCAZAR, R., AHARONI, A., KOPKA, J. & KAPLAN, A. 2017a. Metabolic Flexibility Underpins Growth Capabilities of the Fastest Growing Alga. *Current Biology*, 27, 2559-2567.
- TREVES, H., MURIK, O., KEDEM, I., EISENSTADT, D., MEIR, S., ROGACHEV, I., SZYMANSKI, J., KEREN, N., ORF, I., TIBURCIO, A. F., ALCÁZAR, R., AHARONI, A., KOPKA, J. & KAPLAN, A. 2017b. Metabolic flexibility underpins growth capabilities of the fastest growing alga. *Curr Biol*, 27, 2559-2567.
- TREVES, H., SIEMIATKOWSKA, B., LUZAROWSKA, U., MURIK, O., FERNANDEZ-POZO, N., MORAES, T. A., ERBAN, A., ARMBRUSTER, U., BROTMAN, Y., KOPKA, J., RENSING, S. A., SZYMANSKI, J. & STITT, M. 2020a. Multi-omics reveals mechanisms of total resistance to extreme illumination of a desert alga. *Nature Plants*, 6, 1031-1043.
- WOOD, E. E., ROSS, M. E., JUBEAU, S., MONTALESCOT, V. & STANLEY, M. S. 2022. Progress towards a targeted biorefinery of *Chromochloris zofingiensis*: a review. *Biomass Conversion and Biorefinery*.